# Improved Annual Temperature Cycle Function for Stream Seasonal Thermal Regimes

Daniel Philippus, Claudia R. Corona, and Terri S. Hogue

Hydrologic Science and Engineering Program (Philippus, Hogue), Colorado School of Mines, Golden, Colorado, USA; Department of Civil and Environmental Engineering (Corona), Colorado School of Mines, Golden, Colorado, USA (Correspondence to Philippus: dphilippus@mines.edu).

**This is the accepted version of the following article:** Philippus, D., Corona, C. R., and Hogue, T. S. 2024. "Improved Annual Temperature Cycle Function for Stream Seasonal Thermal Regimes." *Journal of the American Water Resources Association*. DOI: 10.1111/1752-1688.13228, **which has been published in final form at** https://doi.org/10.1111/1752-1688.13228.

**Research Impact Statement:** An improved stream temperature (ST) annual cycle function more accurately captures ST regimes of dynamic climates such as those at high elevation, colder or drier conditions.

**ABSTRACT:** Seasonal regimes of stream temperatures are important for ecological health and function as well as for societal water use and treatment. Seasonal regimes can be captured in the annual temperature cycle (the mean temperature for each day of the year) or in summary statistics such as seasonal mean temperatures, the former of which is the focus of this work. The annual temperature cycle is often characterized as a sine function, which performs satisfactorily for most streams. However, the sine function is unable to capture major seasonal variations, particularly for colder, drier, and high-elevation regions. Seasonal summary statistics are effective for classification but do not capture the full time series, preventing the use of lost time-series information, and lack context for the comparison of trends, hindering distinction between different causes of similar seasonal trends. We propose an improved function called the "three-sine model" to describe the stream annual temperature cycle with higher accuracy and demonstrate its use in two case studies. The three-sine model uses a cosine function over the entire year coupled with two seasonal anomaly sine functions. The three-sine model captures the stream annual

temperature cycle with eight parameters, reveals distinct spatial trends, and outperforms the sinusoidal model for all elevations and ~99% of individual streams. We conclude that this improved approach has the potential to support improved stream temperature analysis and forecasting by capturing detailed seasonal trends in context.

(**KEYWORDS:** stream temperature; thermal regime; annual temperature cycle; seasonality; hydrological data analysis)

## INTRODUCTION

Stream water temperature is a key factor for water chemistry, e.g. dissolved oxygen (Caissie 2006), drinking water treatment (Honey-Rosés *et al.* 2013), and aquatic life, by impacts on species metabolism, behavior, and population growth (Caissie 2006; Poole and Berman 2001). Stream temperature is a central variable in habitat suitability (e.g., Harig and Fausch 2002), degradation (e.g., Poole and Berman 2001), and restoration (e.g., Abdi *et al.* 2021), motivating extensive research on stream temperature at local to national scales (e.g., Booth, D. B. *et al.* 2014; Isaak *et al.* 2020; Maheu *et al.* 2016). Important stream temperature characteristics for ecology and water quality often concern the seasonal pattern of temperature, such as distinct seasonal needs for fish growth and survival (e.g., Caissie 2006; Mochnacz *et al.* 2023) or maximum temperatures for water treatment infrastructure which occur in the summer (e.g., Honey-Rosés *et al.* 2013).

Infrastructure and ecological implications make stream seasonal thermal regimes important to stream management applications, with extensive research ongoing into stream seasonal thermal regime characterization (e.g., Ward 1963; Isaak *et al.* 2020; Maheu *et al.* 2016; Tasker and Burns 1974; Hudson *et al.* 2023). The seasonal thermal regime of streams, in terms of the full cycle of day-of-year mean temperatures (annual temperature

cycle), follows a generally sinusoidal pattern throughout the year (Caissie 2006), with a maximum around Julian day 190-230 (July to August) (Maheu *et al.* 2016) in the northern hemisphere. The annual temperature cycle can be affected by snowmelt and freezing in colder regions (Maheu *et al.* 2016; Isaak *et al.* 2020), but the overall cycle remains approximately sinusoidal during the non-frozen part of the year (Caissie 2006).

The entire annual temperature cycle may not be relevant to a specific concern, and stream management applications based on seasonal thermal regimes often benefit from selection of relevant regime summary characteristics, such as summer temperatures (Honey-Rosés *et al.* 2013) or maximum 30-day mean temperatures (Zeigler *et al.* 2019) and computation or prediction thereof. One approach to summarizing the seasonal thermal regime is to describe a function characterizing mean stream temperatures throughout the year, or the annual temperature cycle. In the literature, the stream annual temperature cycle has often been modeled as a sinusoid (Caissie *et al.* 2005; Caissie 2006; Ducharne 2008; Tasker and Burns 1974; Ward 1963).

Since the 1960s (Ward 1963), the sinusoid model has been used to compress information about stream temperature regimes into two (mean temperature and sinusoid amplitude) or three (with phase) summary numbers that allow for efficient classification and comparison (e.g., Maheu *et al.* 2016). The sinusoid provides a simple and efficient representation of general trends, but, with only two or three coefficients, it may not capture detailed seasonal variations introduced by locally-variable heat exchange considerations such as solar radiation, snowpack, or hydrogeology (Caissie 2006). Thus, studies investigating stream thermal regimes (e.g., Isaak *et al.* 2020; Hudson *et al.* 2023)

often avoid using such a summary of the annual temperature cycle as a whole, instead using separate summary statistics such as mean temperature as a representation of each season. The preference for separate summary statistics stems from the asymmetrical mean temperature patterns across the four seasons (e.g., snowmelt in spring that is not present in autumn), which cannot be captured in a symmetrical sine curve. An example of the implications of non-sinusoidal seasonal patterns is provided by Isaak *et al.* (2020), which developed a classification of Western United States (U.S.) stream thermal regimes based on summary statistics. The classifications of western U.S. streams in Isaak *et al.* (2020) include parameters like variable timing of the beginning of spring (spring onset) which are incompatible with the symmetrical nature of a sine curve. Excluding parameters like spring onset means that the traditional sinusoid model cannot adequately replicate their classification of western U.S. stream thermal regimes, thereby limiting the analysis of patterns identified in Isaak *et al.* (2017a). Furthermore, in Isaak *et al.* (2020), spring onset timing is noted as significantly differing for streams considered "mid-elevation mountain" versus "high mountain" streams (Isaak *et al.* 2020), a difference which can only be captured with summary statistics or an asymmetrical function that addresses the impact of elevation on stream seasonal thermal regimes.

We propose that the sine curve model, typically used to represent seasonal thermal regimes, can be improved to better capture distinct spring and autumn behaviors or variable timing in existing regimes as well as future climate change. Widely-applicable analyses of stream thermal regimes, whether summary statistic-based or as a continuous function, must account for diverse present and future conditions such as snow,

groundwater, lake and reservoir influence (Isaak *et al.* 2020; Hudson *et al.* 2023), all of which may have asymmetrical seasonal impacts.

The purpose of this study is to identify consistent deviations from the sinusoid model and use them to construct a more universally applicable stream annual temperature cycle function for thermal regime analyses, herein called the "three-sine model". Given recognized thermal regime variations in high-elevation environments (Isaak *et al.* 2020), we ask: (1) How can anomalies from a sinusoidal annual temperature cycle for high-elevation streams be quantified in a function, and (2) Do the anomalies reflect a generalizable pattern across the U.S.? We conduct this study by examining daily records of stream temperature across 2,222 U.S. Geological Survey (USGS) gages throughout the U.S. for the period of October 1964 - January 2023 (U.S. Geological Survey, National Water Information System. Accessed August 2023, https://dashboard.waterdata.usgs.gov/). We describe the development of a three-sine model and its improvements and increased accuracy over the traditional sine model and discuss the applications of the three-sine model through analysis of spatial trends.

## METHODS

### *Data Retrieval*

Stream water temperature data were retrieved from the USGS gage network through the National Water Information System (U.S. Geological Survey, National Water Information System. Accessed August 2023, https://dashboard.waterdata.usgs.gov/). Gages were identified and data downloaded using the dataRetrieval package (Cicco *et al.*

2022) in R (R Core Team 2021). Using dataRetrieval, all stream gages with stream temperature observations in each state were listed, and the gages were further screened for at least 365 days of data and available metadata (i.e., elevation, drainage area identification, and drainage area). After filtering, 2,222 gages met the conditions for use across the U.S. (Fig. 1).

Gage characteristics from the retrieved dataset are summarized in Table 1. A large part of the dataset is composed of measurements from gages at lower elevation (e.g., 80% under ~600 m and 50% under ~240 m; Fig. 2) and located in the eastern U.S. (64% <100 West). However, ~27% of gages were located in western mountain ranges of the U.S. (Rocky Mountains from New Mexico to Idaho, Cascade Mountains in the Pacific Northwest, Sierra Nevada in California and Nevada, etc.), the desert southwest of Arizona, New Mexico, and surrounding areas, Alaska, and Hawaii (Fig. 1, Table 2).

*Table 1. Variable ranges in stream temperature dataset*

| Variable (units) | Minimum | Maximum |
|---|---|---|
| Elevation (m) | -4 | 2900 |
| Drainage area ($km^2$) | 0.1 | $2.9 \times 10^6$ |
| Latitude (North) | 20 | 71 |
| Longitude (West) | 67 | 164 |
| Day-of-year mean stream temperature (C) | 0 | 36 |
| Overall mean stream temperature (C) | 0.6 | 28 |

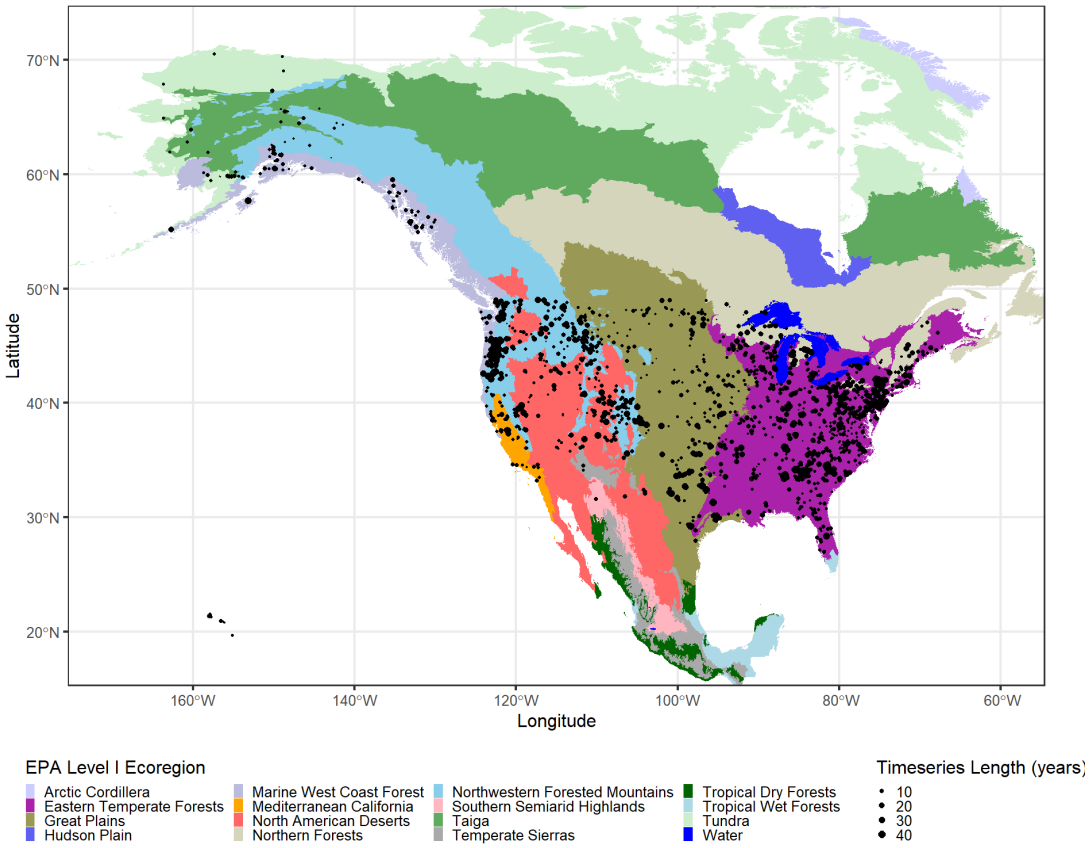


*Figure 1. Distribution and available time-series length of United States Geological Survey (USGS) gages analyzed, shown with Environmental Protection Agency (EPA) Level I Ecoregions (Omernik and Griffith 2014)*

*Table 2. Coverage of only sparsely-gaged (not all gages included) regions and EPA Level I Ecoregions (Omernik and Griffith 2014) of interest.*

*Most stream temperature gages are concentrated east of the 100$^{th}$ Meridian and on the West Coast excluding Alaska (Fig. 1).*

| Region [Type] (as shown on Fig. 1) | Gage Count |
|---|---|
| Northwestern Forested Mountains [Ecoregion] | 303 |
| North American Deserts [Ecoregion] | 177 |
| Alaska [State] | 106 |
| Hawaii [State] | 15 |

*Model Development*

Prior to analysis, the streams in the dataset were evenly-distributed into ten groups herein called "buckets", with each bucket containing 10% of gages, organized by elevation. Organizing the streams by elevation allows the identification of seasonal temperature patterns at higher elevations that may not be apparent overall in a low elevation-dominated dataset (with 80% of gages at <600 m).

Annual temperature cycles organized by elevation bucket (Fig. 2) show that annual temperature cycles at all elevations follow a loosely sinusoidal pattern as indicated in the literature (Caissie *et al.* 2005; Caissie 2006; Ducharne 2008; Tasker and Burns 1974; Ward 1963), but with large deviations at several times of year, particularly at higher elevations. To capture seasonal deviations, the new model was constructed based on the residuals of the annual temperature cycles compared to a best-fit cosine. We focused on residuals to

identify additional terms that would capture the observed variation compared to the established sinusoid model. For the visual inspection of the model design, we used the 31-day centered rolling mean (i.e., roughly monthly, with a centered approach requiring an odd number of days) residual to reduce noise and highlight general trends. Of the annual time-series of residuals, there were four portions with a consistent trend of approximately sinusoidal form. Specifically, residuals tended to be zero or slightly negative around the start of the calendar year, increasing to a local maximum around Julian day 50-100 (winter-high), then decreasing to a local minimum around day 150 (spring-low), and repeating that pattern with a local maximum and minimum near day 210 (summer-high) and day 330 (autumn-low). The autumn-winter and spring-summer pairs of anomalies tended to have similar amplitudes, allowing anomalies to be fitted as two sine functions (autumn-winter, spring-summer) instead of four independent components. Fitting four independent anomaly functions, as one sinusoid each, was tested, but showed worse performance.

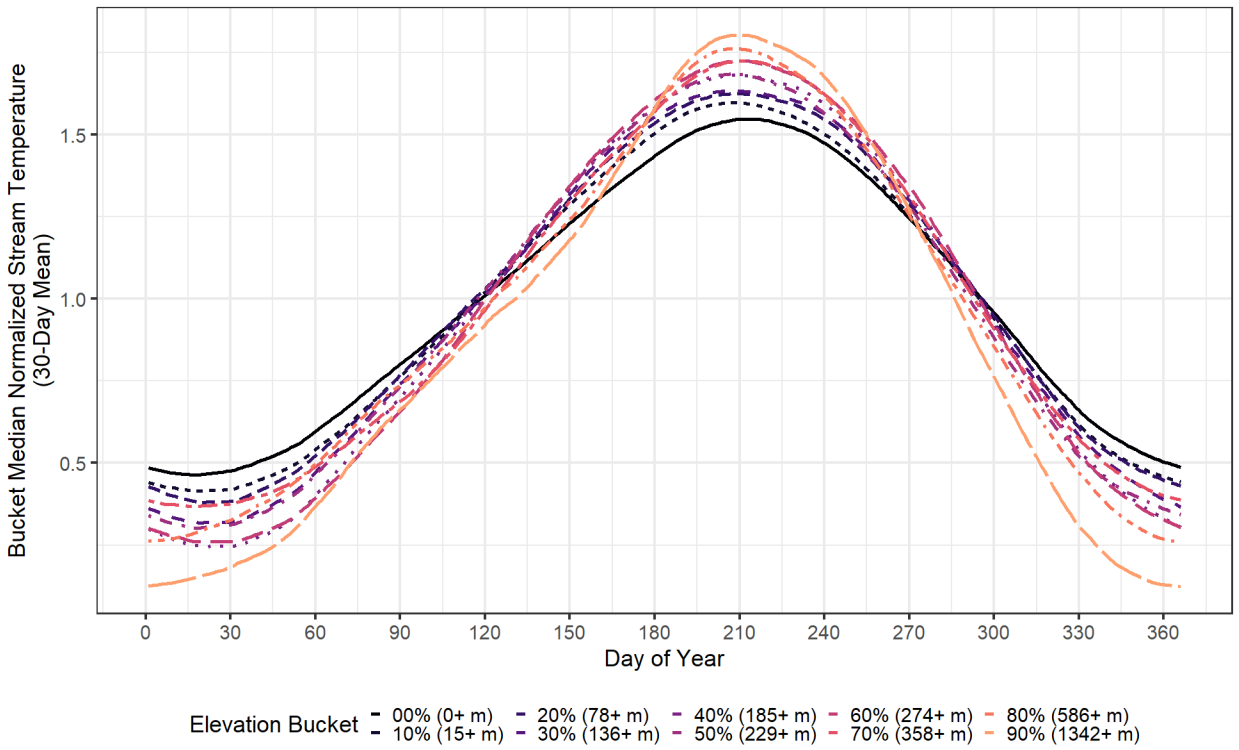


*Figure 2. Observed 30-day rolling mean of the median day-of-year mean temperatures across streams in the United States (US) by elevation bucket*

The baseline sinusoid model (e.g., Caissie *et al.* 2005; Caissie 2006; Ducharne 2008; Tasker and Burns 1974; Ward 1963) is typically specified using the mean annual temperature and the ordinary least squares best fit amplitude of a cosine function. Fitting the baseline model independently of anomaly functions (i.e., spring-summer and autumn-winter sines) and before fitting the latter is necessary in order to identify the days of the year on which the anomaly functions have their maxima and minima, since the anomaly functions are fitted based on residuals from the baseline sinusoid. In the observed data, the maximum temperature, the timing of which sets the phase of the baseline sinusoid,

generally occurred on or about Julian day 210 (late July), which is in agreement with the literature (Caissie 2006). For a maximum on day 210, sinusoidal day-of-year temperature $T_s$ is expressed in terms of day of year $d$, intercept $\overline{T}$, and amplitude $A$ as Eq. 1. For testing the baseline sinusoid alone, erroneous sub-freezing predictions were set to 0 C to ensure that sub-zero predictions did not produce a spurious penalty to model fit.

$$T_s = \overline{T} + A\cos\left((d - 210) \cdot \frac{2\pi}{365}\right) \quad (1)$$

Next, the four identified anomalies (spring, summer, autumn, winter) are fitted with two sine curves corresponding to the autumn-winter and spring-summer anomaly pairs (Fig. 3). First, the phase timing is determined based on local maxima and minima of the annual temperature cycle, using a 31-day rolling mean to reduce noise around the maxima and minima. Timing of anomaly maxima or minima is not consistent across streams due to variable climate characteristics (e.g., snowmelt timing), making it necessary to select the phases for each stream accordingly. Once peak (maximum or minimum) timing is identified, the two sine functions are specified with appropriate phase (Eq. 2) and a period equal to twice the maximum-to-minimum time. Each function is then applied only to a domain of one period and set to zero otherwise. The limited domains allow the two anomaly pairs to have independent amplitudes unaffected by interference between the two sine functions. Finally, the coefficients of the intercept, main cosine, and two anomaly sine functions are fitted using ordinary least squares regression, a common method for identifying optimal coefficients (e.g., Ward 1963). Thus, for two anomaly sine functions with start day $t$, period $\tau$, and best-fit amplitude $a$, we introduce the three-sine model (Fig. 3) with day-of-year mean temperature $T_a$ (Eq. 2):

$$T_a = \overline{T} \quad +A\cos\left((d-210)\cdot\frac{2\pi}{365}\right) \\ -a_1\sin_{t_1,t_1+\tau_1}\left((d-t_1)\frac{2\pi}{\tau_1}\right) - a_2\sin_{t_2,t_2+\tau_2}\left((d-t_2)\frac{2\pi}{\tau_2}\right) \quad (2)$$

Where $\sin_{a,b}(x) = \begin{cases}\sin(x) & x \in [a,b] \\ 0 & otherwise\end{cases}$.

In this fitting method, the two anomaly sine functions are subtracted because the peak in each sine function (autumn, spring) corresponds to a low temperature anomaly (negative residual from the main cosine) and vice versa. This convention allows $a_{1,2}$ to be reported as positive by default.

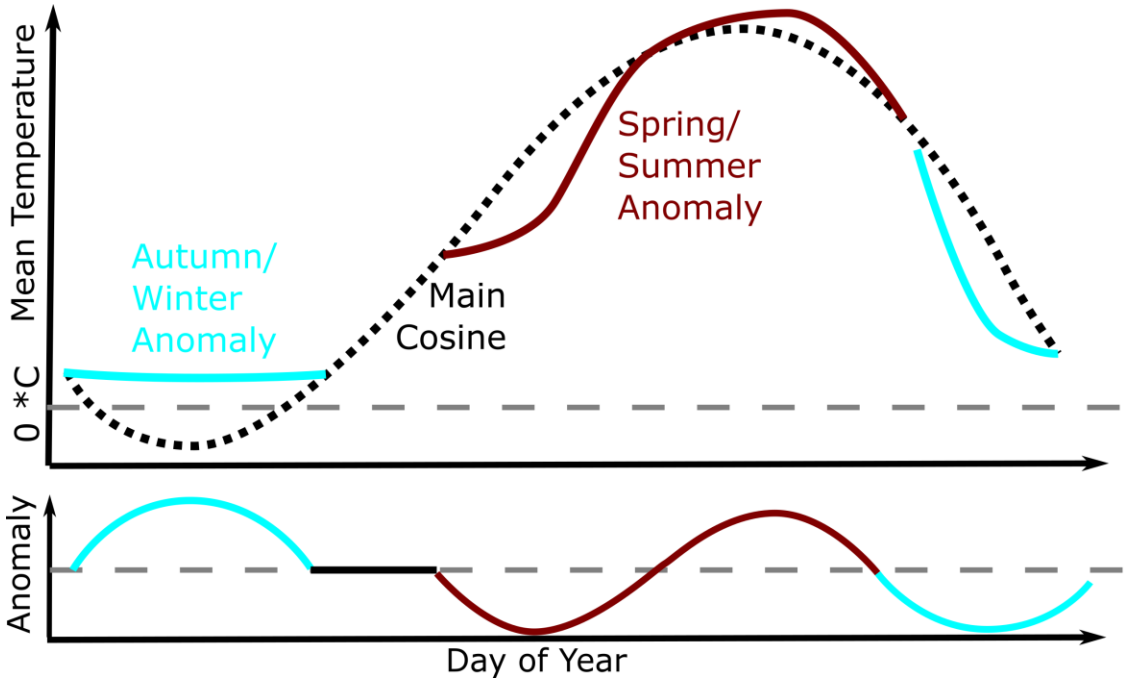


*Figure 3. Conceptual diagram of the three-sine model components, showing the year-long main cosine curve (corresponding to the sinusoid model) as well as the two limited-*

*domain seasonal anomaly pairs and their sum. The diagram shows a generic river not specific to any data source, but would map most closely to a snowy, mountainous watershed.*

*Model Performance Evaluation*

Within the ten elevation quantile buckets (10% of stream gages per bucket) and for individual streams, we obtained the Akaike Information Criterion (AIC) (Akaike 1974) for both the traditional sinusoid model and the three-sine model, computing log-likelihood with the R function logLik (R Core Team 2021). The Akaike Information Criterion compares the performance of a model (in terms of its likelihood) to its complexity (in terms of the number of parameters) and is used to evaluate performance-complexity tradeoffs between multiple models (e.g., Booth, D. B. *et al.* 2014). Thus, the use of AIC as a performance criterion served to assess whether the increased complexity of the three-sine model was justified, though it could not directly evaluate overfitting. We also calculated the statistical significance of the ordinary least squares coefficient of each predictor using the significance test built in to the 'lm' function in R (R Core Team 2021).

A discrete Fourier transform is another approach that can be used to analyze temporal patterns, where the time-series of interest is decomposed into a sum of sinusoidal functions of varying frequencies. Apart from the extraction of a single sinusoid with a one-year period (Maheu *et al.* 2016, equivalent to the traditional sinusoid model except in allowing variable phase), the discrete Fourier transform approach has not been applied to regime classifications. However, additional terms could improve model fitting, potentially making discrete Fourier transforms important for comparison. To compare the three-sine model and discrete Fourier transform performance and model complexity, we also

reconstructed the annual temperature cycle time-series using only a given number of frequencies from the fast Fourier transform (R Core Team 2021) and determined how many components were needed to equal three-sine model performance in terms of median $R^2$ by elevation group.

To test the duration of observed anomaly patterns for both the sinusoid and three-sine models, we used cross-validation, an approach commonly used to prevent overfitting (e.g., Isaak *et al.* 2017a). Specifically, we used five-fold cross-validation (Breiman and Spector 1989) by year, which entailed splitting the dataset for each gage into five partitions, each corresponding to 20% of years (1964-2023), and tested model performance for each partition using a model fitted to the other four partitions (covering 80% of years).

*Spatial Trends*

To characterize spatial trends in stream temperature seasonality, we fitted the three-sine model to streams in a two-by-two degree area around each pair of integer coordinates (e.g., 105 West, 40 North) in the contiguous U.S. (CONUS; excluding Alaska and Hawaii). The two-by-two degree fitting area was selected after testing several area sizes (e.g., five-by-five, one-by-one degree tested, not shown) to smooth out short-distance variations while maintaining high enough resolution to clearly identify anomalous areas. For example, a one-by-one degree area was produced but deemed too noisy to visually identify any local-scale trends, while a five-by-five degree area lumped together highly contrasting regions with region-specific behaviors (e.g., parts of the Rocky Mountains with the Great Plains). The three-sine model parameters (mean temperature; amplitudes: main

cosine amplitude and the two anomaly coefficients; the four anomaly minimum/maximum days) were fitted using day-of-year mean temperatures for all streams in each respective grid cell and reported with the three sinusoid amplitudes normalized to mean annual temperature, allowing for comparison of relative variability in the amplitudes between regions. We then plotted each of the eight parameters to examine geographic patterns. Prominent geographic trends were examined for model artifacts by inspecting the observed annual temperature cycles for similar patterns. We also computed the three-sine parameters for all streams within elevation buckets by intervals of 100 m to show general trends.

## RESULTS

### *Performance Characteristics of Three-Sine Model*

The sinusoid model performed as expected for most gages, with a median $R^2 \sim 0.96$ for mean day-of-year temperature (annual temperature cycle). However, the remaining unexplained variance is capable of shifting seasonal timing and conditions considerably (Fig. 2). When compared, the three-sine model (median $R^2 \sim 0.99$) outperforms the sinusoid model (median $R^2 \sim 0.96$) overall and for all gages in the dataset. By elevation, the median difference between the three-sine and sinusoidal $R^2$ oscillated around 0.02 for the lower 60-70% of gages ($\lesssim$300 m elevation), then increased up to 0.06 for gages at elevations $\gtrsim$1300 m ($\sim$10% of gages). For gages located at high elevation, the performance of the sinusoid model declined (to a median $R^2 \sim 0.93$ for the upper 10%) while the median $R^2$ of the three-sine model remained $\sim$0.99. The constant performance of the three-

sine model and diminishing performance of the sinusoid model suggest that stream thermal behavior shifted more towards the seasonal anomalies (not captured by the sinusoid) and away from the main cosine. This was likely driven principally by an increasing role of snowpack. The AIC was lower (better) for the eight-parameter three-sine model than for the two-parameter sinusoid model in the ten elevation buckets (Fig. 4). For ~98% of individual streams, the three-sine model had a lower (better) AIC than the sinusoid model. Since AIC accounts for model complexity, the consistent and large advantage of the three-sine model in AIC suggests that the increased model complexity is justified.

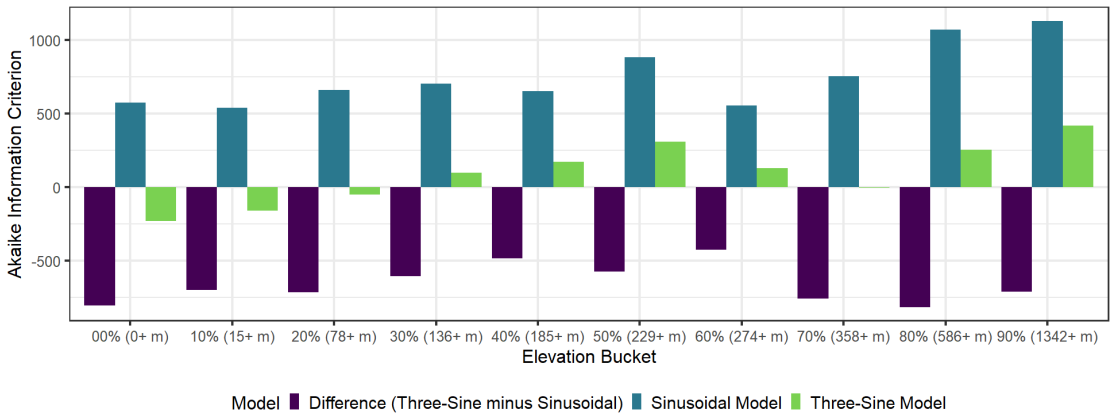


*Figure 4. Comparison of Akaike Information Criterion (AIC; lower is better) for sinusoid model and three-sine model by elevation bucket*

The anomaly pair coefficients identify the magnitude of seasonal anomalies, and the three-sine model differs from the sinusoid model to the extent that anomaly coefficients are nonzero (Eq. 1-2); the two equations are equal if anomaly coefficients $a_1 = a_2 = 0$). To identify nonzero coefficients, we used the probability that each nonzero-fitted coefficient is a result of chance ($p$-value), computed automatically by the R 'lm' function (R Core Team

2021) using the standard error of the coefficient. For this study, the null hypothesis is that each coefficient is zero. Of the two anomaly pair coefficients, the autumn-winter coefficient was statistically significant ($p < 0.05$) for ~95% of individual streams, with $p < 0.001$ for 92% of all streams. The spring-summer coefficient was statistically significant for 68% of streams, with $p < 0.001$ for 63% of all streams. Both coefficients were statistically significant ($p < 0.01$) for all elevation buckets except for the 274-358 m bucket, where $p = 0.054$ for the spring-summer anomaly but the fall-winter anomaly remained statistically significant ($p \approx 0$). For most elevation buckets and most individual streams, both anomaly coefficients had a $p < 0.0001$, indicating a low likelihood of arising by chance.

A discrete Fourier transform using three frequencies (1/year, 2/year, 3/year) had nearly identical performance to the three-sine model for all elevation buckets, with a marginally higher median $R^2$ (by ~0.002). For the Fourier transform, each frequency is a complex number (two components each), in contrast to the real-valued three-sine parameters. Thus, three complex Fourier terms are equivalent in complexity to six real parameters for the three-sine model.

To assess the model's generalizability, we used five-fold cross-validation by year for the 1964-2023 study period. Using cross-validation, the three-sine model outperformed the sinusoid model by a similar margin to overall fit (median $R^2$ difference ~0.03), while both experienced a similar reduction in median $R^2$ of ~0.09 (to 0.87 and 0.90, respectively). This reduction indicates minor variation in the annual temperature cycle from year to year, which a function fitted to other years could not capture. Furthermore, using cross-validation, the performance gap between the three-sine and traditional

sinusoid models widened with higher elevation, with the median increase in $R^2$ rising from 0.01 for gages at 0-500 m elevation to 0.08 for gages at 2500-3000 m elevation.

*Spatial Trends*

Mean annual stream temperature and sinusoid amplitude reflect expected trends from general U.S. geography. For example, mean stream water temperatures, the intercept of the annual temperature cycle function, were higher in southern regions of the CONUS, at lower elevations, and near the Gulf of Mexico (Fig. 5). In contrast, high amplitudes (of the main cosine), which reflect larger temperature swings throughout the year, were identified in areas with colder winters, such as the inland north and the northern Northeast regions of the U.S. (SI Fig. 1).

The new anomaly parameters from the three-sine model revealed geographic distributions not identified by the traditional sine model. For example, for the northern Mountain West (highest elevation streams), the three-sine model captured substantially lower spring temperatures compared to the sine model (Fig. 2). These lower spring water temperatures throughout the northern Mountain West were identified as large spring and summer anomalies, with magnitudes of ~20-40% of local mean stream temperatures (Fig. 6). The lower spring temperature pattern differed from the mean temperature and amplitude patterns captured in both the sinusoid and three-sine models. For example, the largest spring-summer anomaly coefficients (20-40% of mean annual temperatures) near the northern Rocky Mountains (part of the northern Mountain West) aligned spatially with midrange amplitudes (~75-100% of mean annual temperatures; CONUS-wide, most amplitudes ranged from 40-125%) and lower mean temperatures (<15 C).

Similar to the northern Mountain West, parts of the Northeast exhibited large (~20-40% of mean stream temperature) spring-summer anomaly coefficients. However, for the Northeast, the large anomaly coefficients corresponded to some of the lowest mean temperatures and high amplitudes. The autumn and winter anomaly coefficient also had a distinct trend, appearing weaker (<10% of mean stream water temperature) in much of the eastern U.S., and stronger (10-40%) in the West and northern Midwest.

In Fig. 7, the clusters representing seasonality show that timing trends varied across the CONUS. In general, anomaly peaks occurred relatively early in the Northeast and northern Midwest ("Cold North" cluster) and late in the Southeast ("Warm"). The West and much of the Midwest exhibited distinct patterns for each season, which allowed for a reasonable separation into two clusters, "Continental" and "Mountain". Both clusters had mid-range timing (i.e., Julian day) for autumn (day 310-330) and spring (day 140-160), but the summer high arrived early (day 200-205) for Continental sites and later (day 210-240) for Mountain sites, while the winter-high timing had the reverse pattern, occurring around day 80-95 for Continental sites and day 25-40 for Mountain sites. Thus, the four coefficients (mean, amplitude, spring-summer, autumn-winter) and four peak anomaly dates revealed a more distinctive range of trends than the two sinusoid coefficients alone (mean and amplitude).

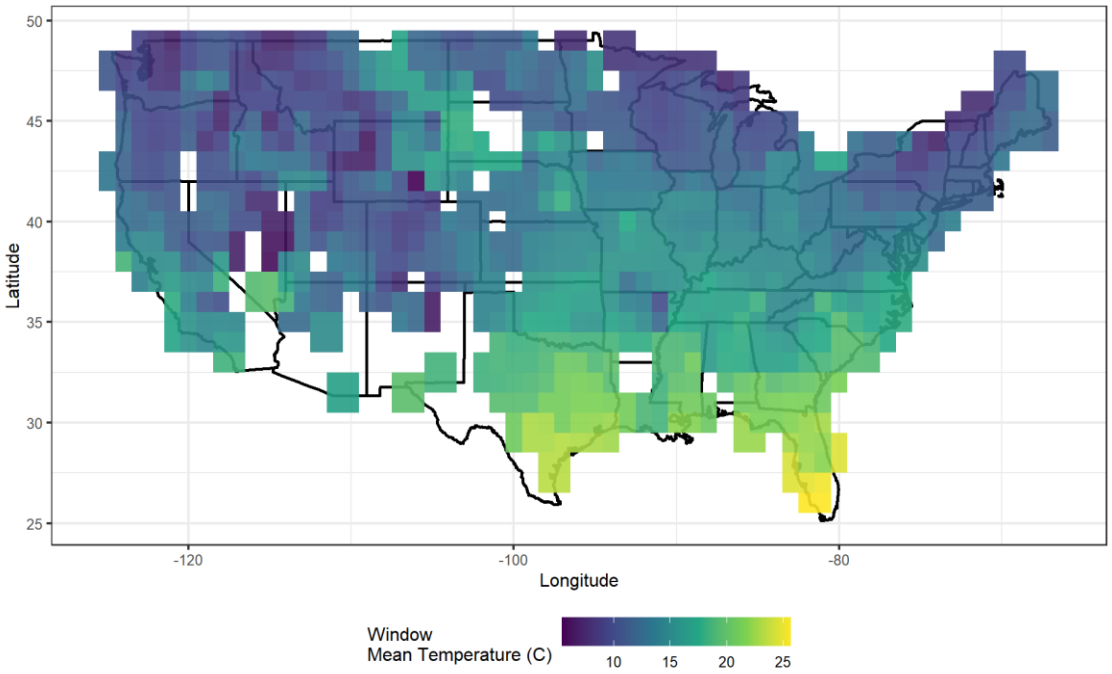


*Figure 5. Mean annual temperature for stream gages in 2-degree windows across the contiguous U.S. (CONUS)*

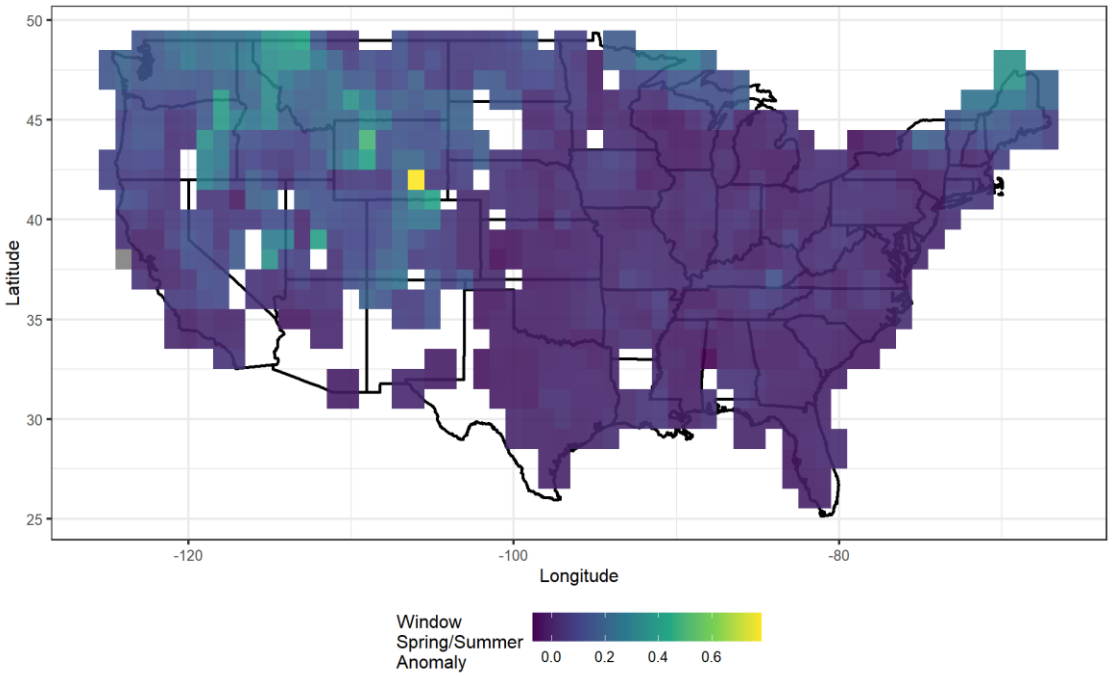


*Figure 6. Magnitude of the spring and summer anomaly coefficient divded by mean annual stream temperature for stream gages in 2-degree windows across the CONUS*

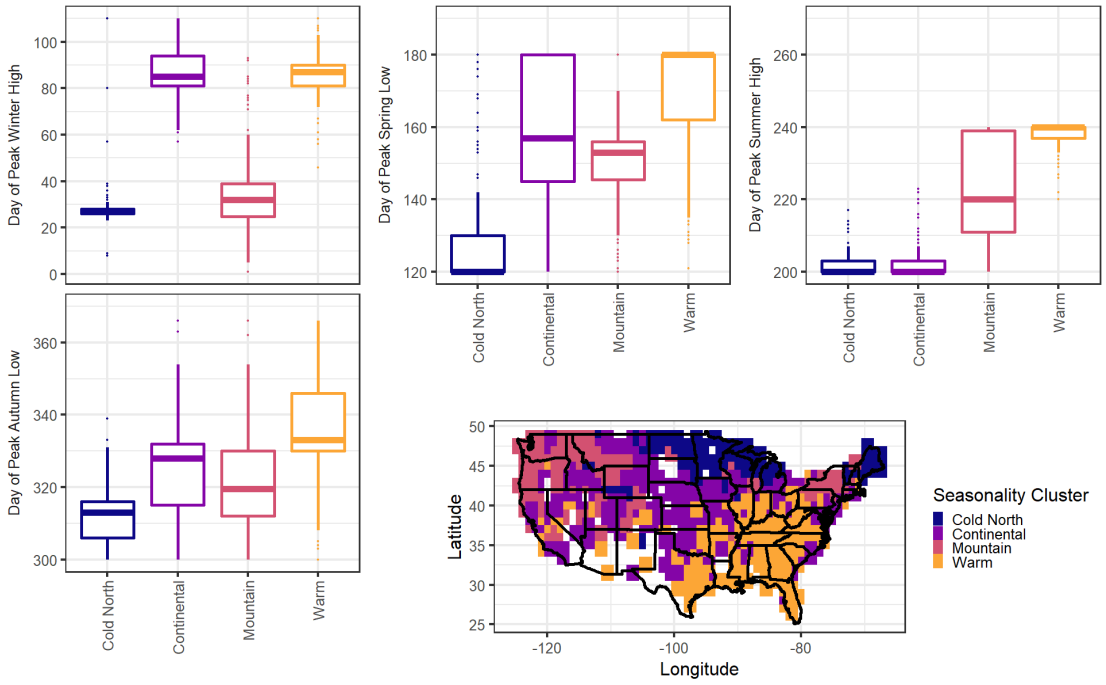


*Figure 7. Anomaly timing ranges for four broad regions of the CONUS. The clusters shown were developed using the hierarchical clustering algorithm implemented in R (hclust) (R Core Team 2021), including all eight seasonality coefficients.*

**Spatial Trends Verification** High values in the two (spring-summer, autumn-winter) anomaly coefficients overlapped in the northern Mountain West (specifically western Montana) and in northern Maine. Due to the overlap, the western Montana and northern Maine sites served as ideal cases for trend-verification across geographic regions. The autumn/winter and spring/summer anomaly coefficients for these regions were 20-40% of mean temperatures. By comparison, Florida (the third region chosen) had anomaly coefficients of less than 10% of mean stream water temperature. Given the contrasting characteristics of the three sites, the difference between the actual annual cycle temperature and a best-fit sinusoid should be discernible in western Montana and northern Maine, but negligible in Florida. Using spatial coordinates, these regions were defined as: 110 to 115 W and ≥45N (western Montana); ≤70 W and ≥45 N (northern Maine); ≤87 W and ≤ 30 N (Florida). Collectively, the three-region comparison represents 58 stream temperature gages with ~270,000 observations covering the years 1975 to 2023.

The two selected regions with large amplitudes, Northern Maine and western Montana, had significantly larger anomalies than Florida (Fig. 8). These large anomalies are observed due to region-specific reasons. Florida showed comparatively small anomalies (up to 1 C in the winter) that were inverted (i.e., winter-low, spring-high, summer-low, autumn-high). Western Montana exhibited large anomalies in the high-elevation structure (Fig. 2). Winter temperatures were comparatively warmer than predicted by the sinusoid model, and the winter was followed by an anomalously cold period in the spring, a fast (~30-day) rise in temperature (~6 C from Julian day 170-200) to a short summer peak, and another anomalously cold period in the autumn.

In Northern Maine, winter temperatures were anomalously high (similar to Montana). In contrast to Montana, however, northern Maine's high winter anomaly is due to a low mean but large variation relative to most of the CONUS. With a large amplitude, the main cosine predicts prolonged subzero temperatures. Instead, observed mean stream temperatures were ~0 C from day ~350-070 (roughly calendar winter), which is reflected by the three-sine model autumn-winter anomaly pair. Subsequently, the stream water temperature in the northern Maine region increased slowly over time (in contrast to Montana), resulting in an anomalously cool early spring for region-specific reasons. This difference is reflected as a comparatively earlier date of the spring low for Maine (day 120). Northern Maine and western Montana exhibited a similar summer-high and autumn-low temperature pattern to each other.

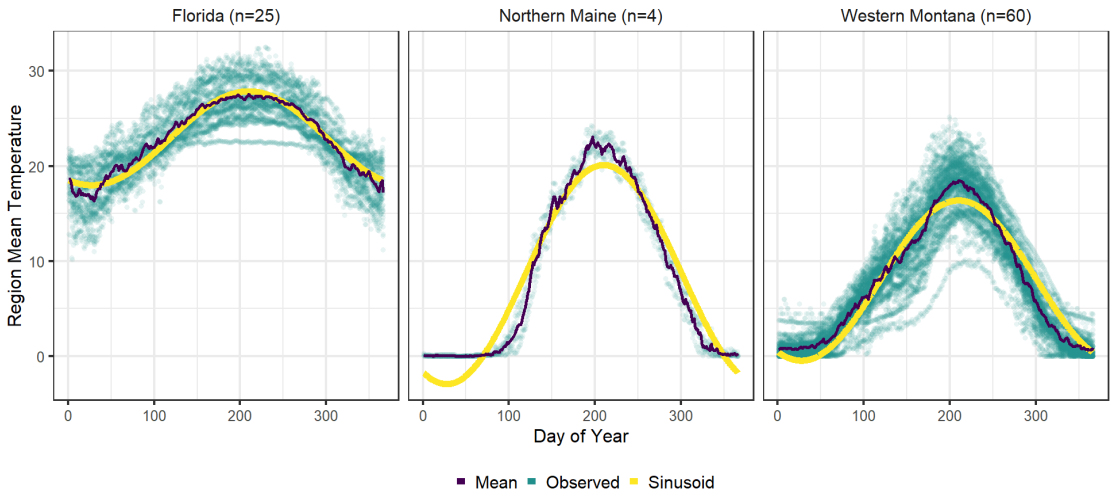


*Figure 8. Observed and sinusoidal stream annual temperature cycles in validation regions of interest; observations include overall mean and individual gages*

**Elevation Stream Temperature Cycle Trends** We observed clear correlations between elevation and all four magnitude parameters: mean temperature, sinusoid amplitude, spring-summer anomaly coefficient, and autumn-winter anomaly coefficient (Fig. 9). With every 1,000 m of increasing elevation, mean stream temperature decreased by ~3 C. The sinusoid amplitude, as a proportion of annual mean stream temperature, increased from ~50% near sea level (~0 m) to 100-125% at >2,000 m elevation. Amplitudes exceeding 100% indicate a winter freeze (with the main cosine predicting sub-zero temperatures). Increasing amplitudes explain part of the rapid rise in the autumn/winter anomaly coefficient, where the main cosine underpredicts the winter temperatures of ≥0 C (e.g., northern Maine, Fig. 8). However, the normalized autumn/winter anomaly coefficient (as a proportion of mean temperature) was larger than the difference between the amplitude and 100% (of mean temperature), indicating that there is a separate anomaly component not explained by freezing conditions.

The spring and summer anomaly coefficient increased more with increasing elevation than the autumn and winter anomaly coefficient. Both anomaly coefficients reached ~30% of mean annual stream temperatures with increasing elevation, especially nearing ~3,000 m. However, at lower elevations, near sea level, the autumn/winter anomaly coefficient started from ~5% of the mean annual stream temperature, whereas the spring/summer anomaly coefficient started from 0%. These elevation trends are apparent in the changing shape of the annual temperature cycles in Fig. 2. We note that there was no obvious trend between timing of each anomaly and elevation.

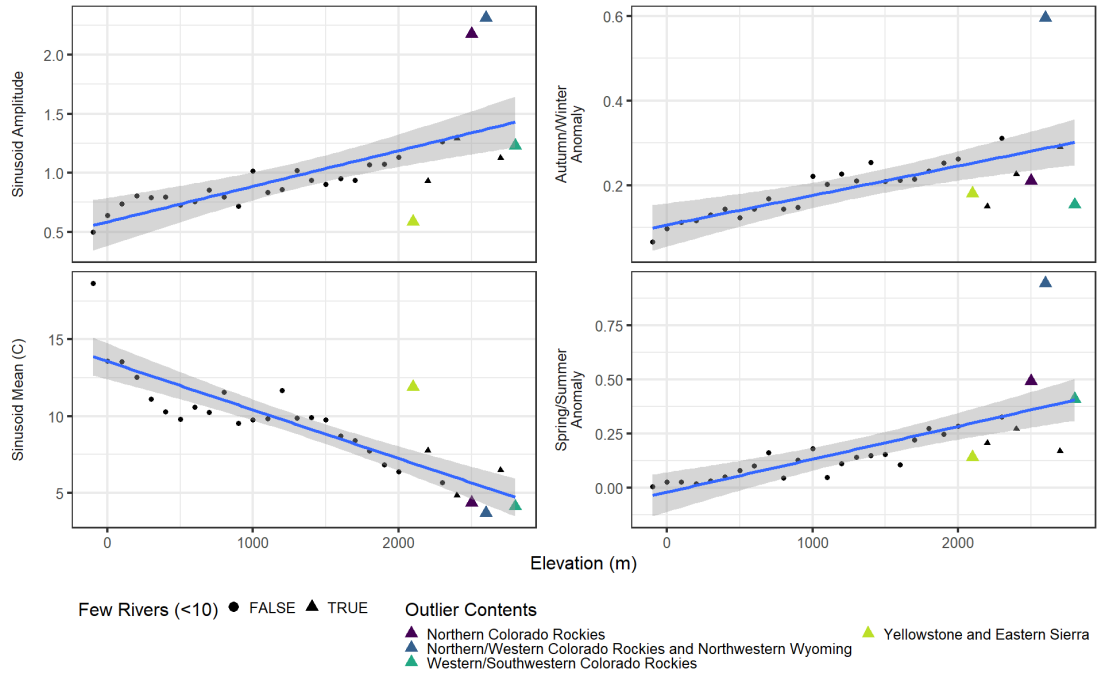


*Figure 9. Trends in median seasonality parameters across rivers within 100-m elevation buckets in the U.S. Amplitude and anomaly magnitudes are normalized to mean stream temperature. Grey shading shows the 95% confidence interval for the best-fit line (blue). Stream gage locations are noted for buckets that are notable outliers in at least one parameter.*

## DISCUSSION

### *General Stream Characterization*

In this study, we demonstrate that there is a consistent pattern in annual temperature cycle residuals relative to the traditional sinusoid model, which can be characterized by two pairs of anomalies: autumn-low/winter-high and spring-low/summer-high. These anomaly pairs are of small magnitude (<20% of mean annual

temperature) but nonzero for most low-elevation streams, and range up to 30-40% of the mean annual temperature in certain regions (e.g., high elevation or arid). The two pairs of anomalies can each be characterized by a sine function over a limited domain (i.e., applied for one period and zero otherwise). The three-sine model improves on the traditional sinusoid model, with better overall accuracy, especially with increasing elevation, and provides more information about stream temperature seasonality. The results from the three-sine model show differences and shifts in seasonal patterns across space and time, whereas the sinusoid model only identifies mean and overall variation. The more detailed function allows spatial and temporal patterns in thermal regimes to be considered in the context of the annual temperature cycle function rather than separately, as has transpired in past research (Isaak *et al.* 2020; Hudson *et al.* 2023) to examine the importance of the seasonal thermal regime in stream processes (Arismendi *et al.* 2013; Olden and Naiman 2010; Poole *et al.* 2004).

We note that the three-sine model does not have a performance advantage over a discrete Fourier transform of similar complexity, but retains a context advantage in the interpretability of the results. Dividing higher-frequency components of the annual cycle into spring-summer and autumn-winter components, which have independent timing and do not interfere with each other, allows seasonal components of the annual temperature cycle to be considered explicitly, as the spatial trend case study showed. This is not the case for the interactions between the first few terms in the Fourier transform, even though they appear to capture seasonal variance similarly, as it is less clear without further processing what the significance is of "a sine-cosine pair with a frequency of 3/year". Even so, it is possible that a discrete Fourier transform approach could map frequencies higher than

1/year to interpretable stream characteristics, which could be an interesting subject for future research.

The traditional sinusoid model, discrete Fourier transform, and three-sine model all consider the annual temperature cycle as a whole. An important advantage of considering the annual temperature cycle as a whole, rather than an expanded set of summary statistics (e.g., seasonal means), is that the annual temperature cycle is not constrained to selected seasonal characteristics, and other data of interest can be extracted from the same parameters. As shown, the three-sine model recreates most annual temperature cycles with excellent accuracy (median $R^2 = 0.99$, including higher elevations) and can be used to identify characteristics of interest such as maximum temperature and seasonal means (e.g., Isaak *et al.* 2020). These parameters are generally unextractable from the traditional sinusoid model if the sinusoid is not a near-perfect fit. Another advantage of the three-sine model is that it places parameters of interest in the context of seasonal patterns overall. This context enables clearer distinction between patterns, such as increasing maximum temperatures as part of a general warming trend versus increasing maximum temperatures with constant mean temperatures - patterns with similar conclusions but separate physical causes and implications. The advantage of increased context is associated with fitting a full annual temperature cycle function (Eq. 2) rather than isolated statistics of interest. On the other hand, the advantage retained by summary statistics is complete flexibility: for example, the three-sine model, being based on a continuous function, would not be able to capture major discontinuities in the temperature cycle (e.g., a near-instantaneous jump or drop in stream temperatures due to anthropogenic activity). The three-sine model also cannot directly represent year-to-year variability, though one could

fit three-sine coefficients for each year individually and compute the variability in the coefficients.

The three-sine model is also capable of describing long-term stream temperature behavior with a continuous function characterized by eight parameters (mean, three sine amplitudes, and four peak anomaly days). Specifically, the model can provide: 1) detailed and clear comparisons between and within locations, 2) the absence of noise and complexity that comes with comparing full time-series, 3) more context (e.g., seasonal temperatures relative to the sinusoidal pattern) than only extracting key values independently, and 4) more detail (e.g., in seasonal variations) than just mean and sinusoid amplitude.

As previously stated, the sinusoid model is generally accepted due to its accuracy for low-elevation streams where observations are most available (Fig. 1). However, our work demonstrates that the accuracy (and therefore usefulness) of the sinusoid model declines markedly even at elevations as low as ~1300 m, an elevation at or above which many areas of environmental concern are located (e.g., ranges of endangered fish species in the U.S. such as Rio Grande Cutthroat Trout (Zeigler *et al.* 2019)). Thus, ecological studies in mountainous regions have used seasonal summary statistics such as August mean temperatures (Isaak *et al.* 2017b) rather than the sinusoid model, and Isaak et al. (2020) proposed further applications using their summary statistic-driven classification. Even some major cities (e.g., Denver, Colorado) are above that elevation threshold, and societal infrastructure introduces its own water temperature concerns such as algae blooms (e.g., Booth, M. 2023). While the deviation from the sinusoid model is strongest at high elevation,

the anomalies are as pronounced in the dry intermountain west, and cold, wet regions in the north, as they are in the high Rocky Mountains (Fig. 6). The performance advantage of the three-sine model with considerably more parameters than the traditional sinusoid runs the risk of overfitting, but this is mitigated by the combination of several factors: sustained performance advantage in cross-validation and AIC; large ratio of observations to parameters (365 to 8); and plausible physical explanations for model terms (e.g., snowpack). For research covering regions that do not follow the typical sinusoidal pattern (Fig. 2), the three-sine model will more accurately assess seasonal temperature trends across diverse geography than the traditional model.

*Spatial Trends*

The geographic trends in anomaly parameters show distinct patterns from the straightforward north-south and Gulf of Mexico-proximity gradients seen in mean stream temperature. In addition to the influence of latitude on stream temperature, the geographic distributions (Fig. 6) suggest that elevation, aridity, and regions of cold and wet climate also play a role, with elevation alone demonstrating strong influence (Fig. 9). The results of this study agree with earlier research (Isaak *et al.* 2020; Maheu *et al.* 2016) which used summary statistic- or sinusoid-based classifications of thermal regime. For example, Isaak *et al.* (2020) included elevation-based classifications (Fig. 9), while the areas of high spring/summer anomaly around the Great Lakes and Maine (Fig. 6) aligned with the "highly variable cool" classification in Maheu *et al.* (2016).

The trends in three-sine parameters with increasing elevation (Fig. 9; increasing amplitude and anomaly coefficients, decreasing mean temperature) show a general

increase in seasonal variation and decrease in mean temperature at higher elevations, which is also captured by the sinusoid model. However, the anomaly parameters provide more detail. Both anomaly coefficients (spring/summer and autumn/winter) rise with elevation, but the spring/summer anomaly rises slightly faster (increasing by ~27% of mean annual temperature from an elevation of 0 - 2800 m, compared to an increase of ~21% of mean annual temperature for the autumn/winter anomaly coefficient). The increase in anomaly coefficients shows that summer and winter temperatures increase compared to the sinusoid prediction, so they both decrease less with increasing elevation than would be implied by the mean temperature and amplitude (Fig. 9). The annual temperature range, on the other hand, widens compared to what the sinusoidal amplitude (which, in the absence of anomalies, is equal to half the difference between maximum and minimum temperatures) would indicate due to larger increase in the spring/summer anomaly coefficient (which increases maximum temperatures) than the autumn/winter anomaly coefficient (which increases minimum temperatures).

In contrast, the spring and autumn temperatures are unaffected by the amplitude of the sinusoid and both temperatures decline faster with increasing elevation than the mean temperature as a result of rising anomaly coefficients. The pattern of decreasing spring and autumn temperatures characterizes the narrowed, asymmetrical annual temperature cycle in Fig. 2. That asymmetrical characterization of the annual temperature cycle at high elevation agrees with the pattern in higher-elevation categorizations from Isaak *et al.* (2020). We note, however, that the annual temperature range observed in this study (Fig. 9) is more expansive than the "moderate annual temperature range" used in Isaak *et al.* (2020). This is because the amplitude herein is normalized to the low mean annual

temperature (i.e., the range at high elevation, as a proportion of mean annual temperature, is wider, relative to other streams, than the range in units of temperature).

*Future Research and Implications*

Our research identified the anomalies relative to the sinusoid model, but there remains a need to investigate the physical causes of the anomalies, which could subsequently allow further improvements to prediction and analysis. Based on this work, we hypothesize that, at high elevations, the cold-spring/warm-summer anomaly pair is influenced by snowmelt patterns. We also hypothesize that, in many streams, the warm-winter anomaly may be a result of streams freezing when the sinusoid predicts subzero water temperatures. Future work could test these hypotheses to better understand the physical causes of the anomalies and variations in their magnitude and timing. For example, Isaak *et al.* (2020) predicted stream thermal regime categories using statistical covariates such as elevation, latitude, annual precipitation, riparian cover, and reach slope, which could serve as proxies for snow, general precipitation regimes, and other physical processes. Models based on such statistical observations could be tested for predictive ability of the full stream annual temperature cycle. In turn, linking physical causes to seasonality terms, coupled with the identification of priority concerns (e.g., excessive summer temperatures) in terms of seasonal components (e.g., mean temperature versus summer anomaly), could inform the selection and planning of restorations (e.g., more efficient restoration methods in Honey-Rosés *et al.* 2013).

The three-sine stream annual temperature cycle model could also be used to replicate and expand on earlier work in stream thermal regime classification by Maheu *et*

*al.* (2016), Isaak *et al.* (2020), and others. For example, the model could be used to analyze the NorWeST dataset for the western U.S. (Isaak *et al.* 2017a, 2020). Such an analysis would be consistent with literature discussion of the importance of delineating stream thermal regimes, rather than using parameters like mean or maximum temperatures alone (Arismendi *et al.* 2013; Olden and Naiman 2010; Poole *et al.* 2004). A major advantage of the three-sine model over an expanded set of summary statistics is that the three-sine model can recreate the entire annual stream temperature cycle with excellent accuracy in most cases (median $R^2$ ~0.99, including at higher elevations) and without being tied to specific seasonal conditions. Further expansions in scope would be supported by testing the three-sine model globally, particularly in tropical and polar climates (which are represented by gages in Hawaii and northern Alaska, but only by a handful of such sites) and, with some modifications to timing, in the Southern Hemisphere.

Building on an understanding of the causes of seasonal anomaly patterns, it would be interesting to predict the annual temperature cycle for ungaged streams. Based on this study, we hypothesize that accurately approximating the entire annual temperature cycle with eight parameters could eliminate the need to model the full annual time-series, thereby allowing for the more efficient creation of a baseline (without weather-driven variation) that describes the typical behavior of a stream. Statistical modeling and forecasting of stream temperatures is a major area of research (e.g., Souaissi *et al.* 2023; Wade *et al.* 2023; Jackson *et al.* 2018; Isaak *et al.* 2017a; McNyset *et al.* 2015), and such a capability could be a powerful tool for seasonal-scale forecasting. This capability would still require modeling of short-term fluctuations, while enabling much of the longer-term variation to be captured simply and efficiently. Modeling summary characteristics rather

than the full time-series was an approach taken by Isaak *et al.* (2020) for modeling thermal regimes. It is possible that such an approach would show no advantage for general stream temperature modeling, but doing so could still capture the baseline, which would be useful for prediction of spatial variability. Another example of the usefulness of the approach is in identifying suitable or concerning seasonal patterns for native fish or lotic species and tracking trends in those patterns (e.g., with climate).

In the context of climate variability, the three-sine model has spatial and temporal applications. For example, Hudson *et al.* (2023) identified cases of a warming spring or autumn without corresponding summer and winter trends. In the context of the three-sine model, these results would likely correspond to weakening spring/summer or autumn/winter anomaly coefficients paired with increasing mean temperatures. The weakening anomaly coefficient would result in a warmer spring or autumn, while the cooling effect on summer or winter would be counteracted by the increasing mean temperatures. While Hudson *et al.* (2023) and similar studies used seasonal temperature means, use of the three-sine model would facilitate expanding the scope of such studies by allowing research to be considered as part of a larger context of overall seasonal thermal regimes while providing a standardized framework for further analyses. The three-sine model itself fits a stationary annual temperature cycle, but, like in other studies of temporal trends in seasonal conditions, it could be fitted to individual years or a moving window of several years, allowing examination of temporal trends in three-sine coefficients.

## CONCLUSIONS

The stream annual temperature cycle has long been characterized as sinusoidal (Caissie *et al.* 2005; Caissie 2006; Ducharne 2008; Tasker and Burns 1974; Ward 1963), but recent research using much more detailed thermal regime summary statistics (e.g., Isaak *et al.* 2020; Hudson *et al.* 2023) indicates the need for a more detailed and flexible stream annual temperature cycle function capable of representing asymmetrical seasonal conditions. We proposed an improvement to the traditional sinusoid model, called the "three-sine" model, and examine how this improved approach shows detailed spatial trends in stream thermal regimes similar to those from summary statistics, but in the form of a continuous function with improved accuracy for approximating the entire annual cycle. The three-sine model sets up an improved framework for investigating stream thermal regime characteristics in context to better support future modeling and analysis for expanding datasets, climate change, and continuing ecosystem management.

## SUPPORTING INFORMATION

Additional supporting information may be found online under the Supporting Information tab for this article: figures showing geographic distributions of all three-sine parameters across the CONUS, expanding on Figs. 5-6.

## DATA AVAILABILITY

The stream temperature data analyzed for annual temperature cycle in this study are publicly available from the U.S. Geological Survey through the National Water

Information System (U.S. Geological Survey, National Water Information System. Accessed August 2023, https://dashboard.waterdata.usgs.gov/) or through the dataRetrieval R package (Cicco *et al.* 2022). The stream temperature data downloaded and analyzed, as well as the R code and R Notebook used to run the analysis (Philippus, Corona, and Hogue 2024), are available in CUAHSI Hydroshare at https://www.hydroshare.org/resource/7d960b7fdfee480895fd845bade1b75a. The code is also publicly available in GitHub at https://github.com/quantum-dan/seasonality, and may be reused, modified, extended, and redistributed under the terms of the GNU General Public License v3.

## ACKNOWLEDGMENTS

This project was supported by the NOAA Cooperative Institute for Research to Operations in Hydrology. Funding was awarded to Cooperative Institute for Research to Operations in Hydrology (CIROH) through the NOAA Cooperative Agreement with The University of Alabama (NA22NWS4320003).

## LITERATURE CITED

Abdi, Reza, Jennifer B. Rogers, Ashley Rust, Jordyn M. Wolfand, Daniel Philippus, Kristine Taniguchi-Quan, Katie Irving, Eric D. Stein, and Terri S. Hogue. 2021. "Simulating the Thermal Impact of Substrate Temperature on Ecological Restoration in Shallow Urban Rivers." *Journal of Environmental Management* 289: 112560. https://doi.org/10.1016/j.jenvman.2021.112560.

Akaike, H. 1974. “A New Look at the Statistical Model Identification.” *IEEE Transactions on Automatic Control* 19 (6): 716–23. https://doi.org/10.1109/TAC.1974.1100705.

Arismendi, Ivan, Sherri L. Johnson, Jason B. Dunham, and Roy Haggerty. 2013. “Descriptors of Natural Thermal Regimes in Streams and Their Responsiveness to Change in the Pacific Northwest of North America.” *Freshwater Biology* 58 (5): 880–94. https://doi.org/10.1111/fwb.12094.

Booth, Derek B., Kristin A. Kraseski, and C. Rhett Jackson. 2014. “Local-Scale and Watershed-Scale Determinants of Summertime Urban Stream Temperatures.” *Hydrological Processes* 28 (4): 2427–38. https://doi.org/10.1002/HYP.9810.

Booth, Michael. 2023. “Are Colorado’s Summer Toxic Algae Blooms Getting Worse? Here’s What to Know.” *The Colorado Sun*. http://coloradosun.com/2023/08/22/colorado-toxic-algae-guide/.

Breiman, Leo, and Philip Spector. 1989. “Submodel Selection and Evaluation in Regression. The X-Random Case.” *International Statistical Review / Revue Internationale de Statistique* 60 (3): 291. https://doi.org/10.2307/1403680.

Caissie, Daniel. 2006. “The Thermal Regime of Rivers: A Review.” *Freshwater Biology* 51 (8): 1389–1406. https://doi.org/10.1111/j.1365-2427.2006.01597.x.

Caissie, Daniel, Mysore G. Satish, and Nassir El-Jabi. 2005. “Predicting River Water Temperatures Using the Equilibrium Temperature Concept with Application on Miramichi River Catchments (New Brunswick, Canada).” *Hydrological Processes* 19 (11): 2137–59. https://doi.org/10.1002/hyp.5684.

Cicco, Laura A. De, David Lorenz, Robert M. Hirsch, William Watkins, and Mike Johnson. 2022. *dataRetrieval: R Packages for Discovering and Retrieving Water Data Available from U.S. Federal Hydrologic Web Services*. Reston, VA: U.S. Geological Survey. https://doi.org/10.5066/P9X4L3GE.

Ducharne, A. 2008. "Importance of Stream Temperature to Climate Change Impact on Water Quality." *Hydrology and Earth System Sciences* 12 (3): 797–810. https://doi.org/10.5194/hess-12-797-2008.

Harig, Amy L., and Kurt D. Fausch. 2002. "Minimum Habitat Requirements for Establishing Translocated Cutthroat Trout Populations." *Ecological Applications* 12 (2): 535–51. https://doi.org/10.1890/1051-0761(2002)012[0535:MHRFET]2.0.CO;2.

Honey-Rosés, Jordi, Vicenç Acuña, Mònica Bardina, Nicholas Brozović, Rafael Marcé, Antoni Munné, Sergi Sabater, *et al.* 2013. "Examining the Demand for Ecosystem Services: The Value of Stream Restoration for Drinking Water Treatment Managers in the Llobregat River, Spain." *Ecological Economics* 90: 196–205. https://doi.org/10.1016/j.ecolecon.2013.03.019.

Hudson, Danielle T., Jason A. Leach, and Daniel Houle. 2023. "Thermal Regimes of Groundwater- and Lake-Fed Headwater Streams Differ in Their Response to Climate Variability." *Limnology and Oceanography Letters* n/a (n/a). https://doi.org/10.1002/lol2.10349.

Isaak, Daniel J., Charles H. Luce, Dona L. Horan, Gwynne L. Chandler, Sherry P. Wollrab, William B. Dubois, and David E. Nagel. 2020. "Thermal Regimes of Perennial Rivers

and Streams in the Western United States." *JAWRA Journal of the American Water Resources Association* 56 (5): 842–67. https://doi.org/10.1111/1752-1688.12864.

Isaak, Daniel J., Seth J. Wenger, Erin E. Peterson, Jay M. Ver Hoef, David E. Nagel, Charles H. Luce, Steven W. Hostetler, *et al.* 2017. "The NorWeST Summer Stream Temperature Model and Scenarios for the Western U.S.: A Crowd-Sourced Database and New Geospatial Tools Foster a User Community and Predict Broad Climate Warming of Rivers and Streams." *Water Resources Research* 53 (11): 9181–9205. https://doi.org/10.1002/2017WR020969.

Isaak, Daniel J., Seth J. Wenger, and Michael K. Young. 2017. "Big biology meets microclimatology: defining thermal niches of ectotherms at landscape scales for conservation planning." *Ecological Applications* 27 (3): 977-990. https://doi.org/10.1002/eap.1501

Jackson, Faye L., Robert J. Fryer, David M. Hannah, Colin P. Millar, and Iain A. Malcolm. 2018. "A Spatio-Temporal Statistical Model of Maximum Daily River Temperatures to Inform the Management of Scotland's Atlantic Salmon Rivers Under Climate Change." *Science of The Total Environment* 612: 1543–58. https://doi.org/10.1016/j.scitotenv.2017.09.010.

Maheu, A., N. L. Poff, and A. St-Hilaire. 2016. "A Classification of Stream Water Temperature Regimes in the Conterminous USA." *River Research and Applications* 32 (5): 896–906. https://doi.org/10.1002/rra.2906.

McNyset, Kristina M., Carol J. Volk, and Chris E. Jordan. 2015. "Developing an Effective Model for Predicting Spatially and Temporally Continuous Stream Temperatures from Remotely Sensed Land Surface Temperatures." *Water* 7 (12): 6827–46. https://doi.org/10.3390/w7126660.

Mochnacz, Neil J., Mark K. Taylor, Margaret F. Docker, and Dan J. Isaak. 2023. "An Ecothermal Paradox: Bull Trout Populations Diverge in Response to Thermal Landscapes Across a Broad Latitudinal Gradient." *Environmental Biology of Fishes* 106 (5): 979–99. https://doi.org/10.1007/s10641-022-01339-0.

Olden, Julian D., and Robert J. Naiman. 2010. "Incorporating Thermal Regimes into Environmental Flows Assessments: Modifying Dam Operations to Restore Freshwater Ecosystem Integrity." *Freshwater Biology* 55 (1): 86–107. https://doi.org/10.1111/j.1365-2427.2009.02179.x.

Omernik, James M., and Glenn E. Griffith. 2014. "Ecoregions of the Conterminous United States: Evolution of a Hierarchical Spatial Framework." *Environmental Management* 54 (6): 1249–66. https://doi.org/10.1007/s00267-014-0364-1.

Philippus, Daniel, Claudia R. Corona, and Terri S. Hogue. 2024. "Stream Temperature Seasonal Thermal Regime Data." Dataset. HydroShare. https://www.hydroshare.org/resource/7d960b7fdfee480895fd845bade1b75a.

Poole, Geoffrey C., and Cara H. Berman. 2001. "An Ecological Perspective on In-Stream Temperature: Natural Heat Dynamics and Mechanisms of Human-CausedThermal

Degradation." *Environmental Management* 27 (6): 787–802. https://doi.org/10.1007/s002670010188.

Poole, Geoffrey C., Jason B. Dunham, Druscilla M. Keenan, Sally T. Sauter, Dale A. McCullough, Christopher Mebane, Jeffrey C. Lockwood, *et al.* 2004. "The Case for Regime-Based Water Quality Standards." *BioScience* 54 (2): 155–61. https://doi.org/10.1641/0006-3568(2004)054[0155:TCFRWQ]2.0.CO;2.

R Core Team. 2021. *R: A Language and Environment for Statistical Computing*. Vienna, Austria: R Foundation for Statistical Computing. https://www.R-project.org.

Souaissi, Zina, Taha B. M. J. Ouarda, and André St-Hilaire. 2023. "Non-Parametric, Semi-Parametric, and Machine Learning Models for River Temperature Frequency Analysis at Ungauged Basins." *Ecological Informatics* 75: 102107. https://doi.org/10.1016/j.ecoinf.2023.102107.

Tasker, Gary D., and Alan W. Burns. 1974. "Mathematical Generalization of Stream Temperature in Central New England1." *JAWRA Journal of the American Water Resources Association* 10 (6): 1133–42. https://doi.org/10.1111/j.1752-1688.1974.tb00633.x.

Wade, Jeffrey, Christa Kelleher, and David M. Hannah. 2023. "Machine Learning Unravels Controls on River Water Temperature Regime Dynamics." *Journal of Hydrology* 623: 129821. https://doi.org/10.1016/j.jhydrol.2023.129821.

Ward, J. C. 1963. "Annual Variation of Stream Water Temperature." *Journal of the Sanitary Engineering Division* 89 (6): 1–16. https://doi.org/10.1061/JSEDAI.0000463.

Zeigler, Matthew P., Kevin B. Rogers, James J. Roberts, Andrew S. Todd, and Kurt D. Fausch. 2019. “Predicting Persistence of Rio Grande Cutthroat Trout Populations in an Uncertain Future.” *North American Journal of Fisheries Management* 39 (5): 819–48. https://doi.org/10.1002/nafm.10320.